Nuclear Engineering and Technology 56 (2024) 275–282

Contents lists available at ScienceDirect

Nuclear Engineering and Technology

journal homepage: www.elsevier.com/locate/net

Original Article

Temperature analysis of extra vessel electromagnetic pump cooling for a Micro nuclear reactor with an electric power of 20 MW

Tae Uk Kang, Hee Reyoung Kim *

Ulsan National Institute of Science and Technology, Department of Nuclear Engineering, Ulsan, 689-798, Republic of Korea

ARTICLE INFO

Keywords:
Electromagnetic pump
temperature analysis
Micro-reactor

ABSTRACT

Lead bismuth eutectic (LBE) is used as coolant for MicroURANUS, a small marine nuclear power plant, and this coolant is transported in the plant by an electromagnetic pump. Given the considerable heat generated by the electromagnetic pump, the cooling of the pump is essential. This study compared air cooling and water-cooling methods and found that the maximum temperatures during air and water cooling were 640 K and 372 K, respectively. These findings were utilized to design an electromagnetic pump with water-cooling. The maximum temperature of the pump was lower than the boiling point of water; thus, the pump did not require a separate pressurization. Consequently, the resistance problem of the coil and the deformation problem of the material caused by generated heat can be solved through water-cooling.

1. Introduction

Micro ubiquitous, rugged, accident-forgiving, non-proliferating, and ultra-lasting sustainer (MicroURANUS) is a small module reactor (SMR) with a target output of 60 MWt [1]. MicroURANUS is a pool-type fast reactor with a six-angle grid core that utilizes lead–bismuth eutectic (LBE) as a coolant because of its chemical stability and ability to achieve a fast neutron spectrum. To maintain nuclear non-proliferation, the primary system of the MicroURANUS is designed to function without pumps, and for 40 years of operation without the substitution or redeployment of the fuel [2]. Heat is removed from the core and transported to the steam generator, which generates electricity, via natural circulation. However, the flowrate generated through natural circulation is insufficient; thus, electromagnetic pumps are used to generate increased flowrates to overcome the pressure drop in the coolant flow area. To solve this problem, the potential of an extra vessel electromagnetic pump (EVEMP) to increase the speed of the coolant passing through the eight steam generators of MicroURANUS has been reported. Since the 1900s, electromagnetic pumps have been investigated for the transport of electrically conductive fluids, such as liquid metals [3]. Electromagnetic pumps transport liquid metals using Lorentz forces generated from the vector product of current and the magnetic field perpendicular to it; thus, they require no rotating component, such as impellers [4,5]. Compared to mechanical pumps, electromagnetic pumps are simpler, smaller in size, and can easily be managed from risk factors, such as corrosiveness of liquid metals of lead and sodium, which are expected to be used as coolant for GEN IV reactors of LFR and SFR [6]. In addition, the pump can prevent the solidification of liquid metal via Joule heating and maintain it in a liquid phase, thus alleviating the need for special heating. However, the electromagnetic pump required for the transportation of high-flow rates liquid LBE in the reactor system exhibits a large input power, and power and current are proportional, which can result in significant heat damage to the core and coil owing to the high temperature. In high-temperature environments, the electrical resistance of the coil becomes high, and this can result in the degradation of the pump performance and material deformation due to increased Joule's heat generation (I^2R), so the coil temperature should be maintained below the maximum permissible temperature (575 K). To this end, the EVEMP of MicroURANUS was thermally analyzed under at a flow rate of 4196 kg/s, developed pressure of 73 kPa, and working temperature of 250 °C.

2. Theoretical approach

The fundamental model of the electromagnetic pump of MicroURANUS is the same as that of an annular linear induction pump (ALIP), which is shown in Fig. 1 [7]. The ALIP is divided into two parts: 1. The primary part, that is, the electromagnet area, consists of internal and external cores and coils. 2. the secondary part is the flow channel, which transports the liquid metal existing between the inner and outer pipes. As shown in Fig. 2, a three-phase alternate current was suitably

* Corresponding author.
E-mail address: kimhr@unist.ac.kr (H.R. Kim).

https://doi.org/10.1016/j.net.2023.09.035
Received 18 April 2023; Received in revised form 28 August 2023; Accepted 30 September 2023
Available online 30 September 2023

Nomenclatures

A	Area [m^2]
$\vec{B}$	Magnetic flux density [T]
C	Specific heat [kJ/kg • K]
$\vec{E}$	Electric field intensity [V/m]
$\vec{F}$	Lorentz force [kg • m/s^2]
h	Heat transfer coefficient [W/m^2 • K]
H	Heat source [W/m^3]
I	Total current [A]
$\vec{J}$	Current density [A/m^2]
k	Thermal conductivity [W/m • K]
m	mass [kg]
$\vec{q}$	Heat flux [W/m^2]
Q	Heat [J]
t	Time [s]
T	Temperature [K]
$\vec{u}$	Fluid velocity [m/s]
w	Frequency [Hz]
ε_0	Electrical permittivity in vacuum [F/m]
μ_0	Magnetic permeability in vacuum [H/m]
ρ	Density [kg/m^3]
σ	Electrical conductivity [1/(Ω • m)]

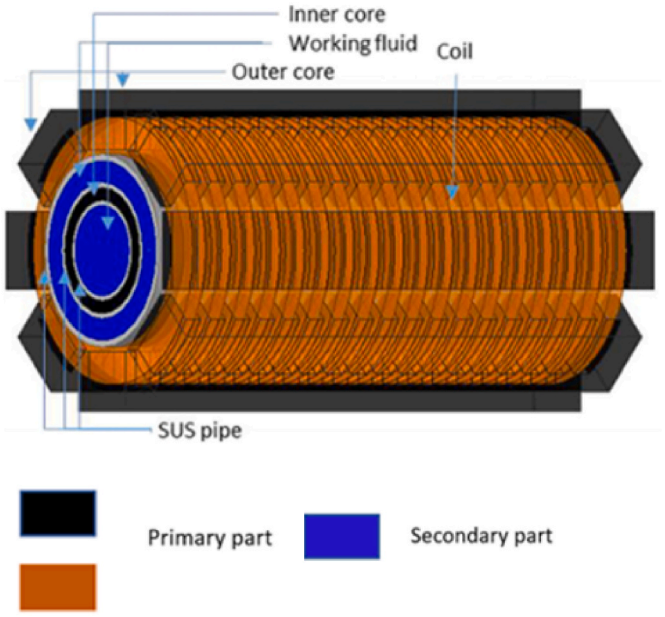

Fig. 1. Conceptual schematic of the electromagnetic pump with the annular linear induction-type pump.

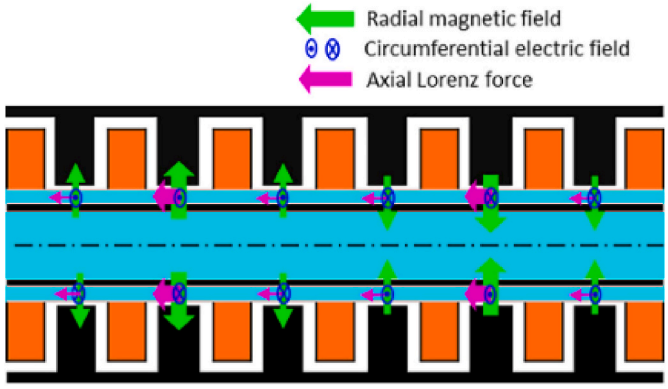

Fig. 2. Operating principle of an electromagnetic pump.

configured into the windings of the copper coils to generate a sinusoidal transverse magnetic field moving in the axial direction. The three-phase alternate current flows, along the inner core and is induced by the E-shaped teeth section of the outer core of the pump, thus, generating a radius-oriented magnetic field. The primary area was composed of high-permeability silicon steel plates (inner core) and low-electrical resistance copper (coil). In the second area, the pipes were composed of SUS 316, which is affected by the reactivity, magnetic flux path distortion, and physical properties of liquid metals [8]. The second area was composed of high-permeability silicon steel plates (inner core) and low-electrical resistance copper (coil). Thus, the temperature was analyzed in the axial and radial directions in the corresponding design, and the design model is shown in Figs 3 and 4. Fig. 3 shows the overall design of the MicroURANUS and the results of the temperature analysis of EVEMP, which is represented by a green dotted square. The temperature of the coils, inner cores, and outer cores, which are components of the EVEMP, was analyzed. Fig. 4 shows the specific design of EVEMP and the simulation was performed based on the corresponding dimensions, where a slot of the EVEMP consists of an exciting coil with 20 turns, as shown in the enlarged view of the part marked A [9]. The simulation of the thermal analysis was performed in 2D. As shown in Fig. 3, EVEMP has a cylindrical shape in a symmetrical state. In addition, as the pump configuration, such as the core and coil, is symmetrical from side to side, the 3D and 2D simulation values were the same.

The strength of the magnetic field was calculated using the Maxwell equation, which consists of Ampere's Law, Faraday's Law, and Gauss's Law, as expressed in equations (1)–(3), and Ohms' law, as expressed in equation (4) [7]. When the three-phase AC current flows from the coil, a time-varying magnetic field was formed along the inner core and outer core of the pump; thus, a current was azimuthally induced in the LBE in the annular cross-sectional duct, where the radial directional magnetic field was formed in the flow channel. Therefore, a Lorentz force was generated from the cross product of the azimuthal current and radial magnetic field. The results of the induced magnetic field were obtained by solving the Maxwell's equations expressed in equations (1)–(3) in cylindrical coordinates. Equation (5), which was derived using equations (1)–(3), was solved coupled with equation (4) to analyze the performance of the electromagnetic pump. To derive the temperature distribution of the EVEMP, equations for heat conduction, heat transfer, and energy transfer were derived, as expressed in equations (6)–(8): heat was obtained using equation (6), substituted for the given conditions in equation (8), and the flow rate was inversely estimated [10]. The pump and internal temperature were calculated at the time of pump operation using COMSOL Multiphysics simulation, and only three coils were analyzed because of their symmetry. The temperature and velocity of the fluid-near solids were calculated, and heat transfer was applied by defining convection heat transfer coefficients and water temperatures. Furthermore, heat transfer equations were applied to the 5 m • 5 m • 5 m space, which is approximately ten times the volume of the water space around the electromagnetic pump, the temperature was set to 300 K. In consideration of the temperature flow condition of the LBE in the flow path, the temperature was set to 520 K, and heat flowed at a speed of 0.5 m/s and was set to a laminar flow.

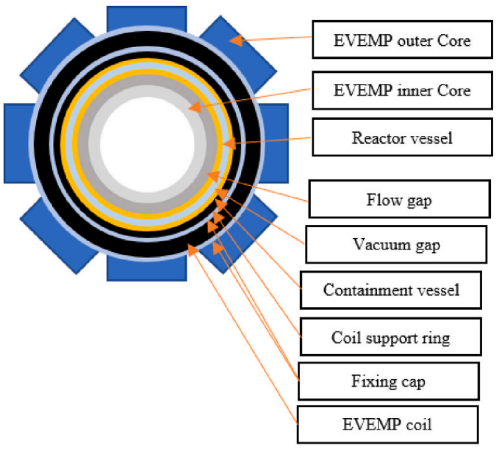

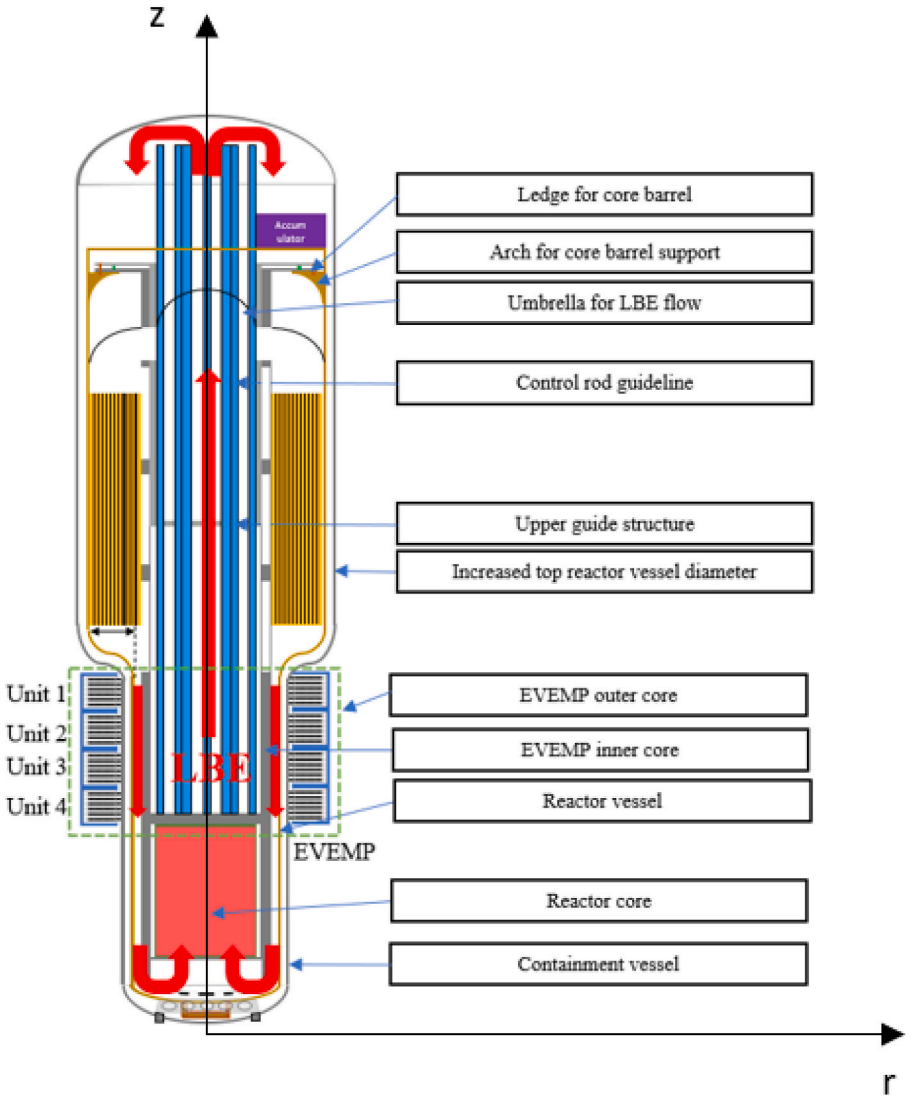

Fig. 3. Design of the MicroURANUS.

$$\text{Ampere's law}: \nabla \times \vec{B} = \mu_0 \left(\vec{J} + \varepsilon_0 \frac{\partial \vec{E}}{\partial t} \right); \quad (1)$$

$$\text{Faraday's law}: \nabla \times \vec{E} = -\frac{\partial \vec{B}}{\partial t}; \quad (2)$$

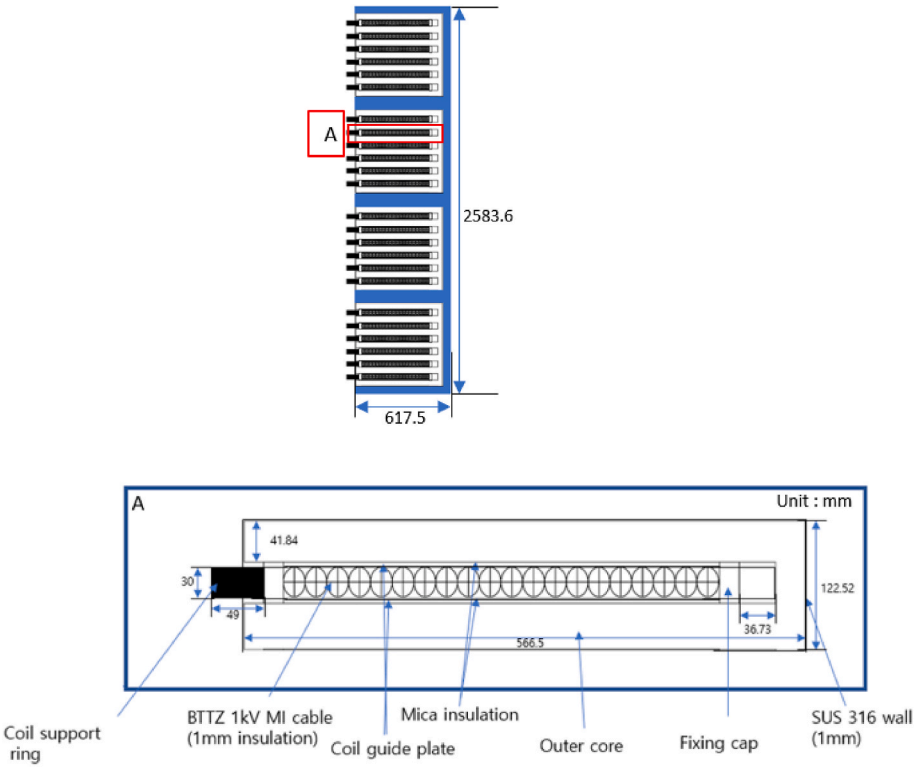

Fig. 4. Specific design of EVEMP.

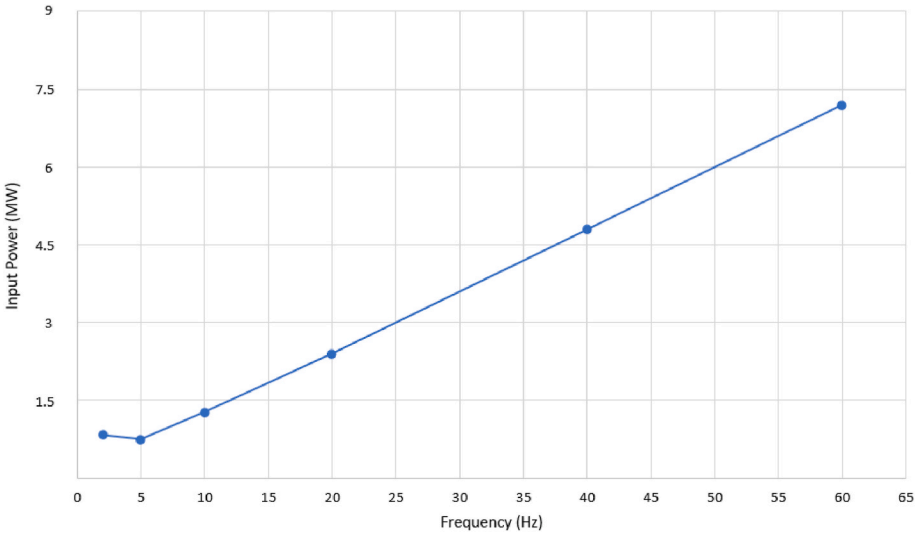

Fig. 5. Input power as a function of the frequency.

$$\text{Gauss's law for magnetism}: \nabla \bullet \vec{B} = 0; \tag{3}$$

$$\text{Ohm's law}: \vec{J} = \sigma\left(\vec{E} + \vec{u} \times \vec{B}\right) \tag{4}$$

$$\nabla^2 \vec{B} = \mu_0 \varepsilon_0 \frac{\partial^2 \vec{B}}{\partial t^2} - \mu_0\left(\nabla \times \vec{J}\right) \tag{5}$$

$$\vec{q} = -\mathrm{k}\nabla \mathrm{T} \tag{6}$$

$$\frac{\mathrm{dQ}}{\mathrm{dt}} = h \bullet A(T_0 - T(t)) \tag{7}$$

$$\rho C\left(\frac{\partial T}{\partial t} + (\vec{u} \bullet \nabla)\mathrm{T}\right) - \nabla \bullet (\mathrm{k}\nabla \mathrm{T}) = \mathrm{H} \tag{8}$$

The EVEMP was designed to yield the highest developed pressure relative to the input power. The number of pole pairs, pump outer core diameter, and input frequency were selected as factors that affect the developed pressure. To reduce the end effect of the electromagnetic pump, a low input frequency was utilized. The diameter of the outer core, number of pole pairs, and flow gap are limited by the geometry. To enter the shield box, the outer core diameter must be within 4 m, and to enter within 2.8 m, which is the maximum height, the pump height is limited to within 2.8 m. As the flow gap was set at 100 mm, the input power according to the frequency was calculated under this condition

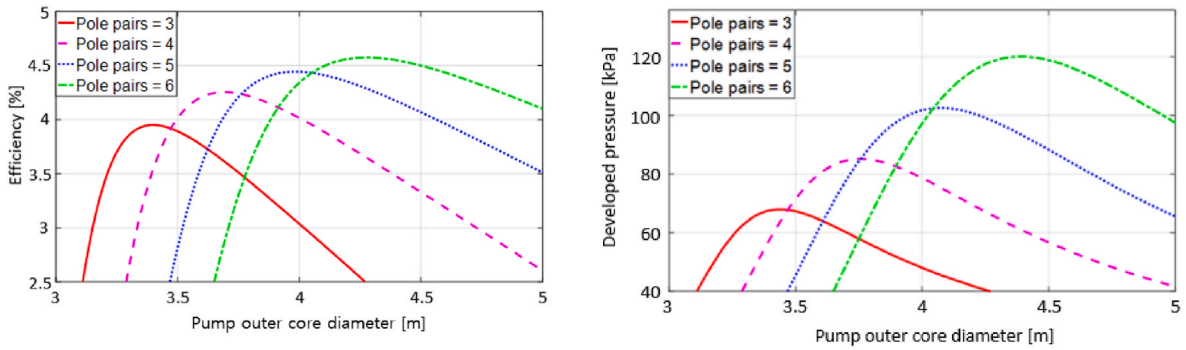

Fig. 6. Efficiency and developed pressure of the EVEMP with a change in the diameter of the pump outer core in different number of pole pairs.

Table 1
Coolant and EVEMP main components properties.

	Thermal conductivity (W/m•K)	heat transfer coefficients (W/m^2•K)	Specific heat (kJ/kg•K)
Water	0.598	1000	4.19
Air	26	3	1.004
Copper	400	–	0.398
SUS 316	16.3	–	0.500
Silicon steel	149	–	0.461

[7]. Fig. 5 shows the power graph as a function of the frequency. The input power was manifested according to the frequency that satisfies the developed pressure condition, and the input power decreases at a frequency lower than 5 Hz, whereas the required input power increased at a frequency higher than 5 Hz. The MicroURANUS investigated was a 20-MW electric power reactor with limited total power, so the advantage of the electromagnetic pump increases with a decrease in the power used by the pump. The electromagnetic pump only needs to satisfy a specific developed pressure (73 kPa). Thus, it can be confirmed that it is efficient to drive the pump at a minimum output power that satisfies the

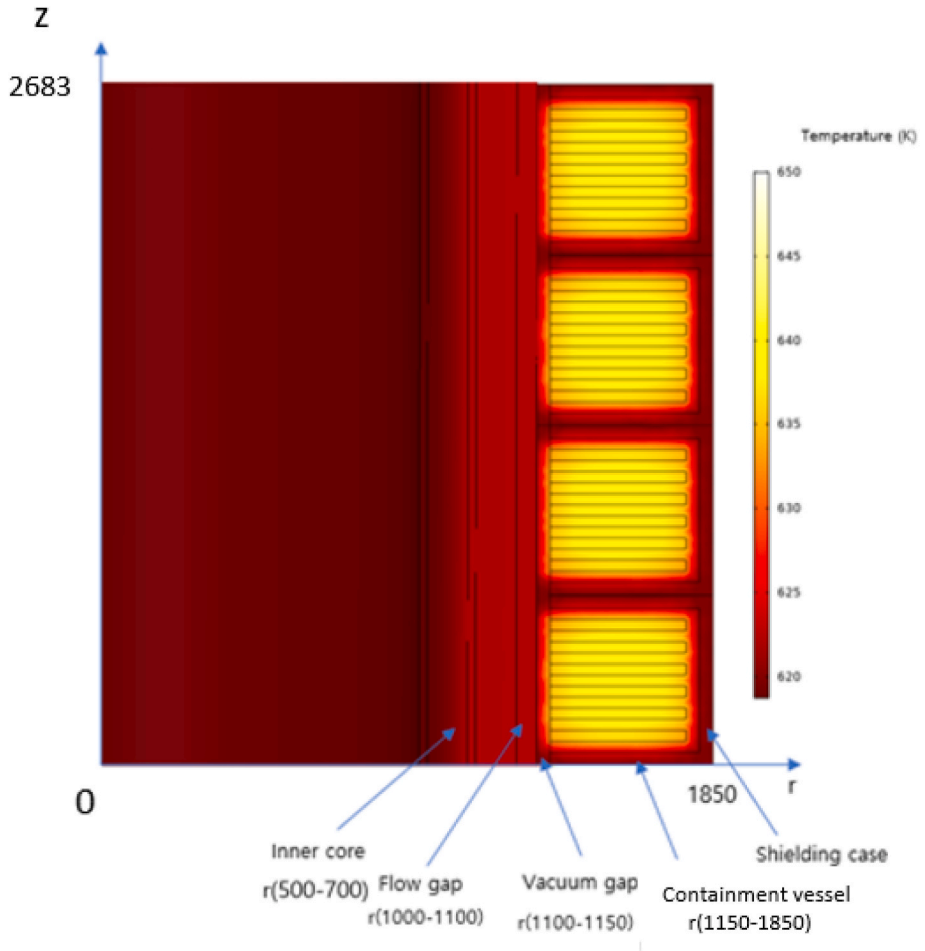

Fig. 7. Temperature distribution of the EVEMP (air cooling).

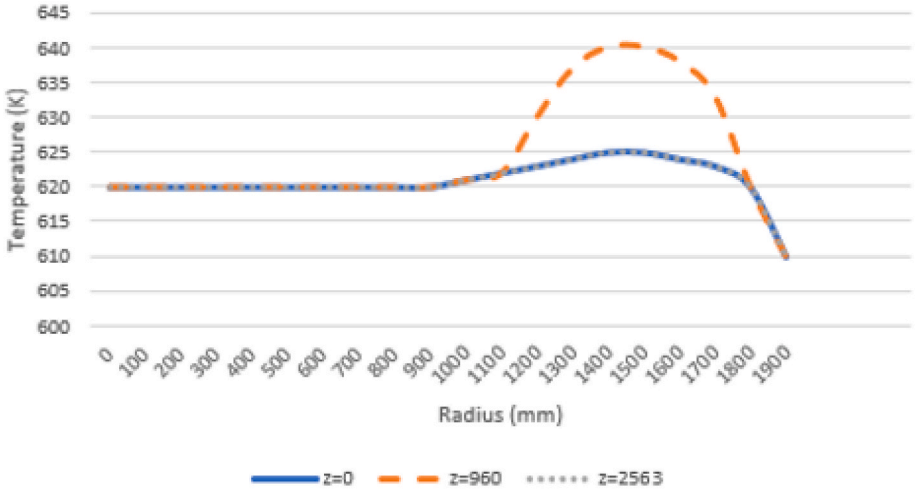

Fig. 8. Temperature distribution of the EVEMP (r-axis, air cooling).

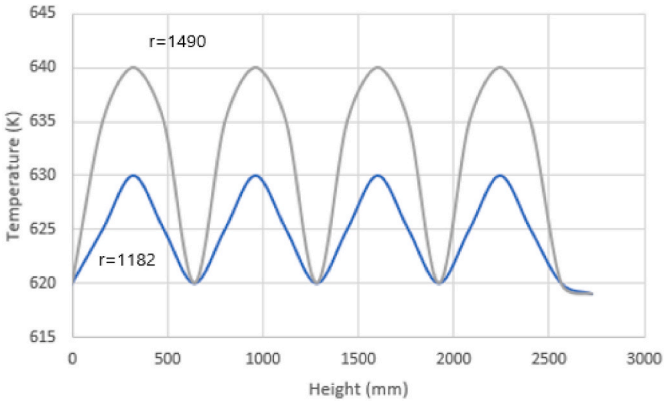

Fig. 9. Temperature distribution of EVEMP (z-axis, air cooling).

developed pressure, and the pressure was optimized at a frequency of 5 Hz. Fig. 6 shows graphs showing the developed pressure and efficiency according to the number of pole pairs and the diameter of the outer core of the pump at 5 Hz [7]. With an increase in the diameter of the outer core of the pump, the efficiency and developed pressure value increased, and then decreased after reaching a peak. If the diameter is too short, the cross section of the tooth reduces in size, and the magnetic field induction was not smooth. If the diameter is too long, the resistance increases, resulting in ohmic loss. Therefore, an optimal diameter is required, and the optimal values in both graphs were observed in the range of 3600–3700 mm. Therefore, considering the thickness of the coil and the size of the reactor, the optimal diameter of the outer core of the pump was determined as 3683 mm. The efficiency and developed pressure values increased as the number of polar pairs in both graphs increased. However, as the EVEMP is located between the steam generator and the core, the pump height was limited to 2500 mm or less. Therefore, a maximum of four pumps can be used as the height of one pole pair is 544.6 mm [7].

The electromagnetic pump was simulated based on the assumption that it was cooled by water at a temperature of 300 K, and heat exchange was performed directly using the pump. The input conditions are: EVEMP current of 1250 A, frequency of 5 Hz, coil windings of 20 turns, and LBE temperature of 520 K. When fluctuations are detected within COMSOL, the grid size was adjusted, so the grid size had no effect on the result.

3. Results and discussion

Equation (9) was used for the first verification through the heat transfer equation. It is a phenomenon in which heat generated by the core and the coil and heat of air or water are exchanged with each other. Therefore, the heat exchange between the two materials can be primarily calculated using equation (9) according to the temperature change. The product of the specific heat, mass, and temperature change of the coil must be equal to the product of the specific heat, mass, and temperature change of water. When this was calculated using the value listed in Table 1, the temperature of the water was approximately 305 K. However, in an actual situation, heat generation proceeds continuously in the coil and core, so the temperature is higher than 305 K; thus, the heat generated over time was calculated using COMSOL Multiphysics. The LBE enters the outer annular path at the bottom of the reactor (next to the core) and is cooled by the heat exchanger, after which it returns to the channel near the electromagnetic pump. In addition, when I^2R and equation (7) were used for the calculation, about a temperature of approximately 372 K was obtained when the outer area of copper and the heat transfer coefficients of water were considered.

$$Q = Cm\triangle T \tag{9}$$

Fig. 7 shows the temperature distribution when the electromagnetic pump was cooled using the air-cooling method. Heat was generated in the coil and the core, and the temperature of the shielding case was relatively low because several parts of the case were in contact with air. The maximum and minimum temperatures of the pump under air cooling was 640 and 620 K, respectively. Fig. 8 shows the temperature distribution and the maximum and minimum temperature points in the r-axis and z-axis. The maximum temperature at points z = 960 and r = 1490 was 641 K, which reduced to approximately 610 K in the shielding case part, where the effect of air cooling was most prominent. Consequently, a low temperature was formed at the lower and upper portions of the electromagnetic pump. Fig. 9 shows a graph of the temperature distribution along the z-axis. The highest and lowest temperatures were observed at points r = 1490, 1182 and 1850, respectively. In addition, a relatively high temperature was observed in the coil and the core where heat is generated.

The overall temperature distribution of the MicroURANUS is shown in Fig. 10. For the water cooling, the EVEMP was cooled at 300 K in the water. The temperature of the outer parts of the outer core, which are in direct contact with water, was relatively low. In contrast, the temperature was relatively high in parts that were not in direct contact.

The temperature inside the MicroURANUS was maintained at approximately 620 K, and was observed to decrease rapidly owing to the

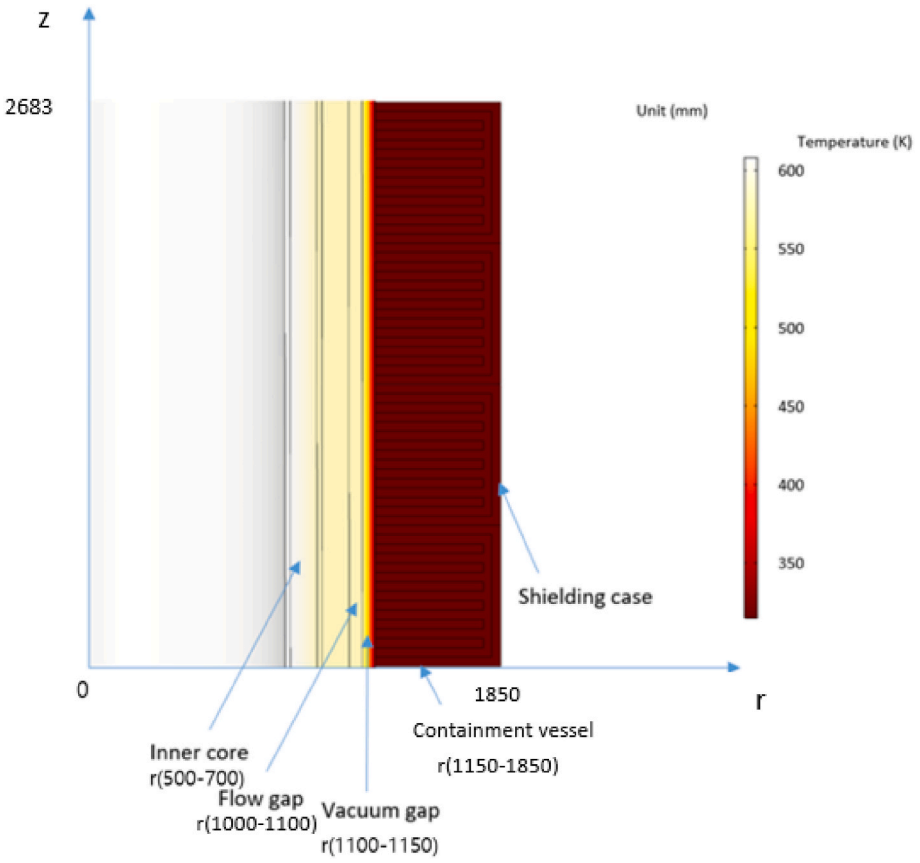

Fig. 10. Temperature distribution of EVEMP.

vacuum gap, which acted as an insulator. As expected, a high temperature of 370 K or above was formed in the center of the coil and outer core. In addition, the temperature in the outer part of the outer core, where water directly touches and cooling was performed smoothly, was relatively low.

Figs. 11 and 12 show the temperature distribution in the r-axis and z-axis of the EVEMP. In the r-axis, 1182 to 1900 are points corresponding to the outer core, and can be confirmed in Fig. 10, and a graph is derived accordingly. The temperature difference in the z-axis was not significant, and the maximum temperature (approximately 372 K) was observed at z = 1320. As the maximum temperature of the outer core is below the boiling point of water, no separate pressurization is required. In addition, as the coil's maximum permissible temperature was approximately 570 K or higher, there is no problem with the material properties. The temperature at r = 1182 was higher than the temperature at r = 1850. The point where r = 1182 exists only for heat transfer to the containment vessel, but the point where r = 1850 was directly affected by water cooling. There was a difference of approximately 10 K between the center and the outside of the core. The temperature of the inner core was well maintained at a temperature of 600 K because the vacuum gap serves as an insulator. As the maximum permissible temperature of stainless steel 316 was approximately 1000 K or more, it was confirmed that there was no problem with the material characteristics of the inner core. The results revealed that the EVEMP maximum

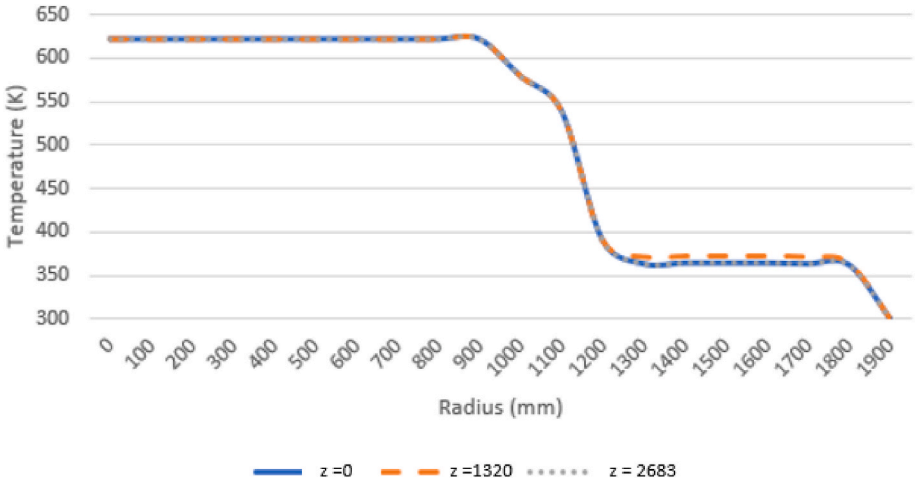

Fig. 11. Temperature distribution of EVEMP (r-axis, water-cooling).

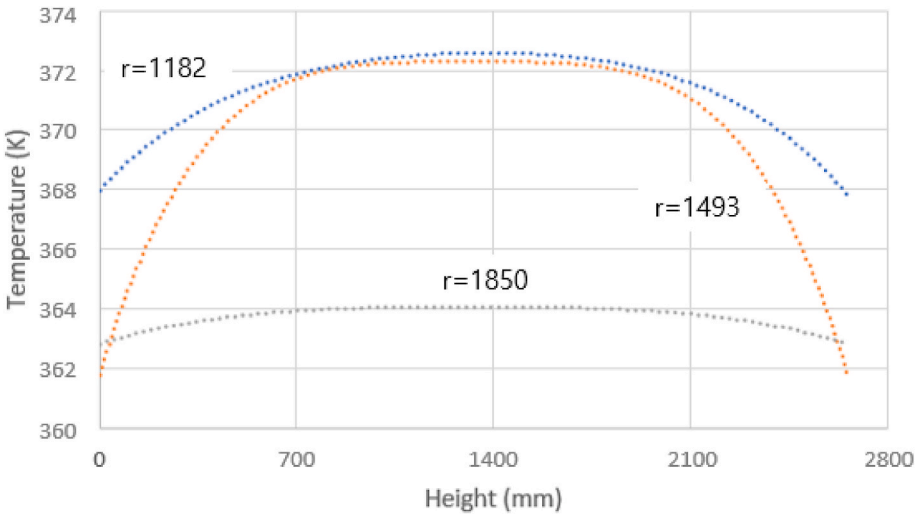

Fig. 12. Temperature distribution of EVEMP (z-axis,water-cooling).

temperature when water-cooling was performed was 372 K, whereas the EVEMP minimum temperature with air-cooling was 620 K. The reduction in the temperature by water-cooling could fundamentally prevent the problems caused by the generated heat, such as deformation and performance degradation.

4. Conclusions

In this study, the temperature distribution of the electromagnetic pump of MicroURANUS, a small marine nuclear power plant, was analyzed. The results revealed that the maximum temperature when the air-cooling method is used was 640 K, which is higher than the maximum temperature when the water-cooling method is used (approximately 270 K). Water cooling was selected because continuous high temperature could damage the pump and the entire reactor. The maximum temperature of the coil and core was confirmed to be 372 K at a current of 1250 A, frequency of 5 Hz, and coil windings of 20. The temperature of the part directly in contact with water was confirmed to be lower than the temperature inside the core. As the maximum temperature was lower than the boiling point of water, no additional pressurization is required, and the use of water-cooling during the operation of the EVEMP was confirmed to be capable of preventing the performance degradation problem caused by generated heat.

Declaration of competing interest

The authors declare the following financial interests/personal relationships which may be considered as potential competing interests: Hee Reyoung Kim reports financial support was provided by Korea Institute of Energy Technology Evaluation and Planning.

Acknowledgement

This work was supported by the Korea Institute of Energy Technology Evaluation and Planning and the Ministry of Trade, Industry & Energy (MOTIE) of the Republic of Korea (grant no. 20214000000410).

References

[1] S.M. Kim, J.H. Cho, I.S. Hwang, The development of LBE integral test loop, HELIOS and tests by using HELIOS, in: Transactions of the Korean Nuclear Society Autumn Meeting, 2011.
[2] H.R. Kim, Y.B. Lee, A design and characteristic experiment of the small annular linear induction electromagnetic pump, Ann. Nucl. Energy 38 (5) (2011) 1046–1052.
[3] K. Aizawa, Y. Chikazawa, S. Kotake, K. Ara, R. Aizawa, H. Ota, Electromagnetic pumps for main cooling systems of commercialized sodium-cooled fast reactor, J. Nucl. Sci. Technol. 48 (3) (2011) 344–352.
[4] A.M. Andreev, B.G. Karasev, I.R. Kirillov, A.P. Ogorodnikov, V.P. Ostapenko, G. T. Semikov, Results of an experimental investigation of electromagnetic pumps for the BOR-60 facility, Magnetohydrodynamics 4 (93) (1978) e100.
[5] A. Andreev, V.G. Danilin, B.G. Karasev, I.R. Kirillov, Choice of construction schemes of electromagnetic pumps for atomic energy stations with fast reactors, Magnetohydrodynamics 18 (1) (1982) 81–84.
[6] G.A. Baranov, V.A. Glukhikh, I.R. Kirillov, Calculation and Design of Liquid-Metal MHD Induction Machines, 1978. Moscow Atomizdat.
[7] T.U. Kang, J.S. Kwak, H.R. Kim, Optimization of an extra vessel electromagnetic pump for Lead–Bismuth eutectic coolant circulation in a non-refueling full-life small reactor, Nucl. Eng. Technol. 54 (10) (2022) 3919–3927.
[8] K. Bessho, S. Yamada, M. Nakano, K. Nakamoto, A new flux concentration type electromagnetic pump for FBR, J. Magn. Magn Mater. 112 (1–3) (1992) 419–422.
[9] UNIST, MINERVA technical report, MicroURANUS-FSAR- 5 (2022) 6R0.
[10] A. Oto, N. Naohara, M. Ishida, T. Kuroki, K. Katsuki, R. Kumazawa, Sodium-immersed self-cooled electromagnetic pump design and development of a large-scale coil for high temperature, Nucl. Technol. 110 (2) (1995) 159–167.